

Update: Cardiac Imaging (III)

Role of Imaging Techniques in Percutaneous Treatment of Mitral Regurgitation

Chi-Hion Li,^{a,b,*} Dabit Arzamendi,^b and Francesc Carreras^a^a Unidad de Imagen Cardíaca, Servicio de Cardiología, Hospital de la Santa Creu i Sant Pau, Barcelona, Spain^b Unidad de Hemodinámica, Servicio de Cardiología, Hospital de la Santa Creu i Sant Pau, Barcelona, Spain

Article history:

Available online 24 February 2016

Keywords:

Mitral regurgitation

Mitral repair

Transesophageal echocardiography

Cardiac computed tomography

Palabras clave:

Insuficiencia mitral

Reparación mitral

Ecocardiografía transesofágica

Tomografía computarizada cardíaca

ABSTRACT

Mitral regurgitation is the most prevalent valvular heart disease in the United States and the second most prevalent in Europe. Patients with severe mitral regurgitation have a poor prognosis with medical therapy once they become symptomatic or develop signs of significant cardiac dysfunction. However, as many as half of these patients are inoperable because of advanced age, ventricular dysfunction, or other comorbidities. Studies have shown that surgery increases survival in patients with organic mitral regurgitation due to valve prolapse but has no clinical benefit in those with functional mitral regurgitation. In this scenario, percutaneous repair for mitral regurgitation in native valves provides alternative management of valvular heart disease in patients at high surgical risk. Percutaneous repair for mitral regurgitation is a growing field that relies heavily on imaging techniques to diagnose functional anatomy and guide repair procedures.

© 2016 Sociedad Española de Cardiología. Published by Elsevier España, S.L.U. All rights reserved.

Papel de las técnicas de imagen en el tratamiento percutáneo de la insuficiencia mitral

RESUMEN

La insuficiencia mitral es la valvulopatía más prevalente en Estados Unidos y la segunda en Europa. Una vez se establecen los síntomas o produce una repercusión significativa en la función cardíaca, la insuficiencia mitral grave tiene un pronóstico adverso con tratamiento médico. A pesar de ello, no se opera hasta la mitad de los pacientes con insuficiencia mitral grave sintomática por edad avanzada, disfunción ventricular y otras comorbilidades. Se ha demostrado que la cirugía obtiene mayor supervivencia a las insuficiencias mitrales orgánicas por prolapso, pero no se ha podido demostrar un beneficio clínico de intervenir insuficiencias mitrales funcionales. En este escenario, la reparación percutánea de la insuficiencia mitral nativa permite intervenir la valvulopatía en pacientes con alto riesgo quirúrgico. La reparación percutánea de la insuficiencia mitral es un campo en expansión con gran dependencia de las técnicas de imagen tanto para el diagnóstico de la anatomía funcional que reparar como para guiar el procedimiento.

© 2016 Sociedad Española de Cardiología. Publicado por Elsevier España, S.L.U. Todos los derechos reservados.

Abbreviations

3D: 3-dimensional

Cardiac CT: cardiac computed tomography

CT: chordae tendineae

LVOT: left ventricular outflow tract

MR: mitral regurgitation

MV: mitral valve

TEE: transesophageal echocardiography

INTRODUCTION

Mitral regurgitation (MR) is the most prevalent valvular heart disease in the United States and the second most prevalent in Europe.^{1–3} Competent mitral valve (MV) function requires the synchronization of several structures to direct blood flow from the atrium to the ventricle in diastole and vice versa in systole. Primary MR is organic failure of the structures that form part of the mitral apparatus. The most frequent etiology of primary MR used to be rheumatic disease but is now degenerative valve disease.^{2,3} Secondary or functional MR is due to subvalvular apparatus distortion or dysfunction due to ventricular enlargement or remodeling, or ischemia.⁴

Patients with severe MR have a poor prognosis with medical therapy once they become symptomatic or develop signs of

* Corresponding author: Servicio de Cardiología, Hospital de la Santa Creu i Sant Pau, Mas Casanovas 90, 08041 Barcelona, Spain.

E-mail address: CH.PedroLi@gmail.com (C.H. Li).

significant cardiac dysfunction (ventricular dysfunction, pulmonary hypertension, or recurrent atrial fibrillation).^{3,5–8} However, as many as half of these patients are inoperable because of advanced age, ventricular dysfunction, or other comorbidities.⁹ Studies have shown that surgery increases survival in patients with organic MR due to valve prolapse^{5,10} but has no clinical benefit in those with functional MR.¹¹

In this scenario, percutaneous repair for MR in native valves provides alternative management of valvular heart disease in patients at high surgical risk.¹² Percutaneous repair for MR is a growing field that relies heavily on imaging techniques to diagnose functional anatomy and guide repair procedures.

Echocardiography is the primary imaging technique used to evaluate cardiac valves due to its high spatial-temporal resolution, availability, portability, and cost-effectiveness. Transesophageal echocardiography (TEE) is the gold standard in mitral leaflet guidance procedures due to many years of experience with mitral valve ultrasound studies. However, TEE has a restricted field of view, and as a result, multidetector cardiac computed tomography (cardiac CT) has been developed, which permits a comprehensive assessment of the mitral valve apparatus.

The different percutaneous repair interventions for MR are based on surgical techniques, including leaflet plication (MitraClip), annuloplasty (Carillon, Mitralign, Accucinch, Cardioband), neo chordae (NeoChord, V-Chordal), and percutaneous bioprosthesis implantation (CardiAQ, Fortis, TIARA, Tendyne).^{13–15} In Europe, MitraClip, Carillon, and NeoChord have marketing authorizations. MitraClip is currently the most widely-used device, with more than 25 000 implantations worldwide and more than 270 cases in Spain.¹⁶

MITRAL VALVE ANATOMY

Knowledge of normal MV anatomy is essential to understand MV functioning and the mechanisms that lead to valve regurgitation, and to identify findings observed in different imaging techniques.

The mitral valve apparatus is composed of a fibrous annulus at the atrioventricular junction where the valve leaflets are attached, and a subvalvular apparatus composed of chordae tendineae (CT) and papillary muscles (PM) that insert into the myocardium in the left ventricle (LV).

Mitral Annulus

The MV annulus is described as a saddle-shaped fibrous structure. Its peaks are furthest from the ventricular apex and are located anteriorly (at the “riding horn”) and posteriorly, and its valleys are located medially and laterally, at the commissures.^{17–19} The mitral valve is attached to the annulus. The annulus provides atrioventricular electrical isolation.

The presence of a complete ring of connective tissue encircling the atrioventricular junction is very rare.²⁰ A thickened, fibrous band acts as a hinge at the aortomitral junction, between the right and left fibrous trigones. This discontinuous membranous band extends along the atrioventricular junction and is the site where the posterior leaflet and left atrium are attached²¹ (Figure 1).

Valve Leaflets

The mitral valve consists of a continuous veil-like structure inserted around the mitral annulus. The free edge of this veil has several indentations or clefts.²² Two of these indentations are

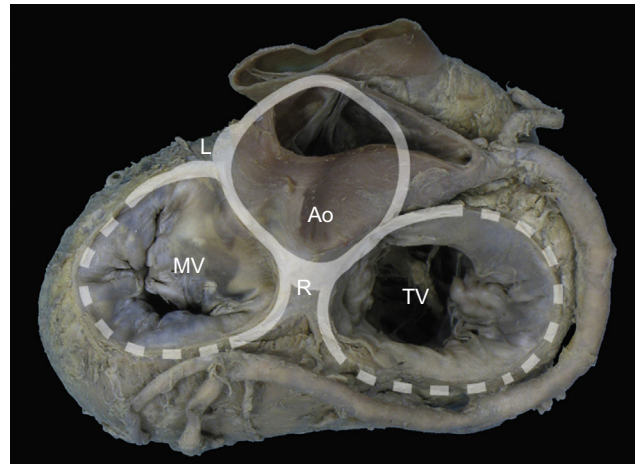


Figure 1. Mitral annulus. Macroscopic view of the base of the heart showing the mitral annulus in relation with the fibrous skeleton (denoted in grey by the aortic and tricuspid annuli) through the right and left fibrous trigones and the aortomitral junction, between the fibrous trigones. Ao, aorta; L, left fibrous trigone; MV, mitral valve; R, right fibrous trigone; TV, tricuspid valve.

positioned in such a way that the structure is divided into 2: the anterior or aortic leaflet, and the posterior or mural leaflet. These 2 main indentations are known as the anterolateral and posteromedial commissures and are characterized by having a clear, translucent central zone, and no distal rough zone. The PMs point toward the commissures.²²

The anterior or aortic leaflet is large, triangular, with few or no indentations. Its atrial surface has a rough, crescentic ridge occupying 1 cm of the distal free edge of the leaflet. The ridge defines the leaflet line of closure and its thickness is due to abundant chordal insertions in the ventricular surface in this area. A clear, translucent zone is distinguished beyond the rough zone, followed by a zone near the base for chordae attachment^{22,23} (Figure 2).

The posterior or mural leaflet is shorter than the anterior leaflet and has a wider attachment to the atrioventricular annulus. The indentations along the free edge give it a scalloped appearance, which varies greatly among individuals. The Carpentier nomenclature²⁴ is used to describe the different scallops or segments: P1 is the most lateral scallop, adjacent to the anterior commissure; P2 is the middle or central scallop, and P3 is the most medial scallop, adjacent to the posterior commissure. The corresponding part of the anterior leaflet located opposite each scallop is named similarly: A1, A2, and A3, respectively. The posterior leaflet has 3 zones: a rough zone, where the line of the leaflet closure is located, a clear or membranous zone, and a basal zone.

Chordae Tendineae

The CT are thin, fibroelastic strings²⁵ that originate from the PMs or directly from the ventricular wall and insert into the ventricular surface of the MV (true CT), or connect between PMs or with the ventricular cavity (false CT). On average, 25 CT insert into the MV and most branch out.²⁶ Two main groups of chords are distinguished by their insertion site and branch location:

- Commissural chordae: These 2 CTs arise from the PM tips and branch out radially like the struts of a fan. They insert into the free edge of the commissures. Commissural chordae are 0.7–1 mm thick and 12–14 mm long.
- Leaflet chordae:

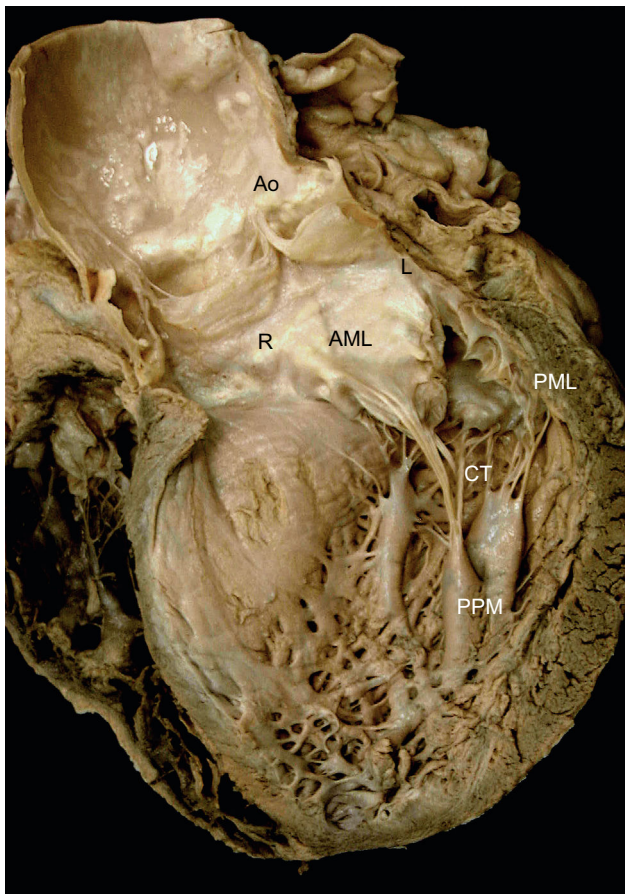


Figure 2. Mitral valve apparatus. Macroscopic view of a long axis slice of the heart through the anterior wall and aortic valve, without the anterior papillary muscle and its chordae tendineae. Note the relation between the anatomic structures and mitral apparatus anchoring to the ventricle via the papillary muscles. Note also how the chordae tendineae insert into the rough zone of the anterior leaflet ventricular surface and extend toward the aorta through the aortomitral junction, with the right and left fibrous trigones on either side. AML, anterior mitral leaflet; Ao, aorta; CT, chordae tendineae; L, left fibrous trigone; PML, posterior mitral leaflet; PPM, posterior papillary muscle; R, right fibrous trigone.

– About 9 CTs insert exclusively into the distal, rough zone of the anterior leaflet. Typically, each chord splits into 3 soon after its origin from the PM. One inserts into the free edge of the leaflet, 1 beyond the free edge in the same rough zone, and an intermediate one inserts between the 2. On average, these chordae are 0.84 mm thick and 17.5 mm long. Two chordae are particularly thick (1.24 mm) and they insert into the ventricular surface of the line of coaptation between the 4 and 5 o'clock positions (on the posteromedial side) and between the 7 and 8 o'clock positions (on the anterolateral side). These chordae are termed struts and were present in more than 90% of the hearts examined in the study by Lam et al.²⁶

– Three types of CT insert into the posterior leaflet. The most characteristic ones are basal chordae that originate directly from the ventricular wall or from small trabeculae carneae. They are sometimes missing altogether and may vary considerably in number, but, on average, 2 basal chordae can be found. Similarly to the anterior leaflet CTs, 10 chordae insert into the rough zone of the posterior leaflet, although they are generally thinner and shorter (0.65 mm and 14 mm, respectively), and 2 others insert into the indentations, adopting a similar radial branching disposition to the commissural chordae.

Papillary muscles

Papillary muscles are specialized cones of LV myocardium. The muscle tissue transitions to MV connective tissue by means of the CT. The free edge of the leaflets are anchored to the ventricle by means of the PMs, which are located in the apical and middle segments of the LV and are aligned with the commissures (Figure 2). Usually, a single PM connects to the anterolateral commissure. In more than 60% of cases, 2 or 3 muscles (or 1 muscle with 2-3 heads) connect to the posteromedial commissure.²³ The anterior PM usually has a dual blood supply, from the left anterior descending coronary artery and branches of the circumflex artery. The posterior PM depends on a single blood vessel, usually the right coronary artery, although the circumflex artery is sometimes responsible for blood supply.⁴ This single-vessel dependence contributes to posterior PM vulnerability to ischemic dysfunction and lesions.

FUNCTIONAL ANATOMY IN MITRAL REGURGITATION

Various mechanisms contribute to the etiology of final functional MV incompetence.²⁷ Carpentier classified 3 functional types of mitral regurgitation^{24,28} from a surgical view, according to leaflet motion:

- Type I: normal leaflet motion. Functional mechanism in cases of annular dilatation and leaflet perforation.
- Type II: excess leaflet motion. Secondary to chord elongation and prolapse; may be associated with chord rupture and leaflet eversion (flail).
- Type III: restricted leaflet motion.
 - IIIa: restricted motion in systole and diastole, typically resulting from infiltrative, mainly rheumatic conditions.
 - IIIb: restricted motion in systole only, typically resulting from ischemic heart disease.

TECHNICAL ASPECTS OF IMAGING TECHNIQUES

Imaging assessment of the cardiac valves requires high temporal resolution to reduce artifacts caused by cardiac and respiratory motion.²⁹ Technically, the temporal resolution of a

Table 1
Technical Aspects of Imaging Techniques

	Fluoroscopy	Echocardiography	CT	MRI
Temporal resolution, ms	7.5-33	15-60	75-135	20-50
Spatial resolution, mm	0.3-1.2	0.6-1	0.4-0.6	1-2
3D reconstruction	No	Yes	Yes	No
Field of view	Unrestricted	Restricted	Unrestricted	Unrestricted

3D, 3-dimensional; CT, computed tomography; MRI, magnetic resonance imaging.

moving object can be defined as the minimum separation in time that a technique is able to visualize. Temporal resolution is therefore measured in milliseconds. Table 1 compares the technical characteristics of the main imaging techniques used to assess cardiac valves vs fluoroscopy, which is the leading technique for percutaneous interventions.

Echocardiography and cardiac magnetic resonance imaging (cardiac MRI) have a higher temporal resolution than cardiac CT. Data acquisition protocols are the main differentiating factor, because cardiac CT requires a quarter or half gantry spin (depending on whether a single or double X-ray tube is used), while echocardiography and cardiac MRI emit ultrasound or radiofrequency pulses, respectively, to acquire images. Three-dimensional (3D) echocardiography and cardiac MRI can also average different heart cycles to improve temporal resolution.^{30–36}

Spatial resolution is the minimum distance that a technique is able to distinguish as 2 different structures. Again, imaging techniques differ considerably in spatial resolution specifications. The best spatial resolution in echocardiography, for example, is achieved when the measured object is in line with the ultrasound beam, close to the transducer and in the area of maximum focus. Under these optimal conditions, spatial resolution is 0.6–1 mm. In cardiac MRI, cine (balanced steady-state free precession) sequences give a maximum spatial resolution of 1–2 mm, while in cardiac CT the range is 0.4–0.6 mm in all 3 dimensions (giving isotropic data) and does not depend on the area of interest, which is ideal for 3D data reconstruction.^{29,37}

These technical aspects, together with availability and data acquisition time factors, influence the role of different imaging techniques in valve assessment and repair guidance. At present, echocardiography (and fluoroscopy) are the leading imaging techniques in implantation guidance, and cardiac CT is the leading imaging technique in intervention planning.^{38–41}

ECHOCARDIOGRAPHIC-GUIDED PERCUTANEOUS REPAIR FOR MITRAL REGURGITATION: MITRACLIP

MitraClip System

The surgical leaflet plication described by Alfieri has simplified native valve repair in MR, using a technique that is independent of the regurgitation mechanism itself.^{42–44} The simplicity and versatility of this technique permit a less invasive approach, initially performed through robotics⁴⁵ and then percutaneously.

The first percutaneous interventions with the Mobius suture system (Edwards Lifesciences Inc.; Irvine, California, United States)⁴⁶ were unsuccessful. In 2003, St. Goar et al⁴⁷ published the first promising results with successful MitraClip deployment in 12 out of 14 pigs. In the 2 remaining animals, the clip detached from one of the leaflets, highlighting the need for echocardiographic monitoring of the grasping step.

MitraClip (Abbott Vascular; Menlo Park, California) is a triaxial catheter system with an implantable clip at the tip. It consists of a

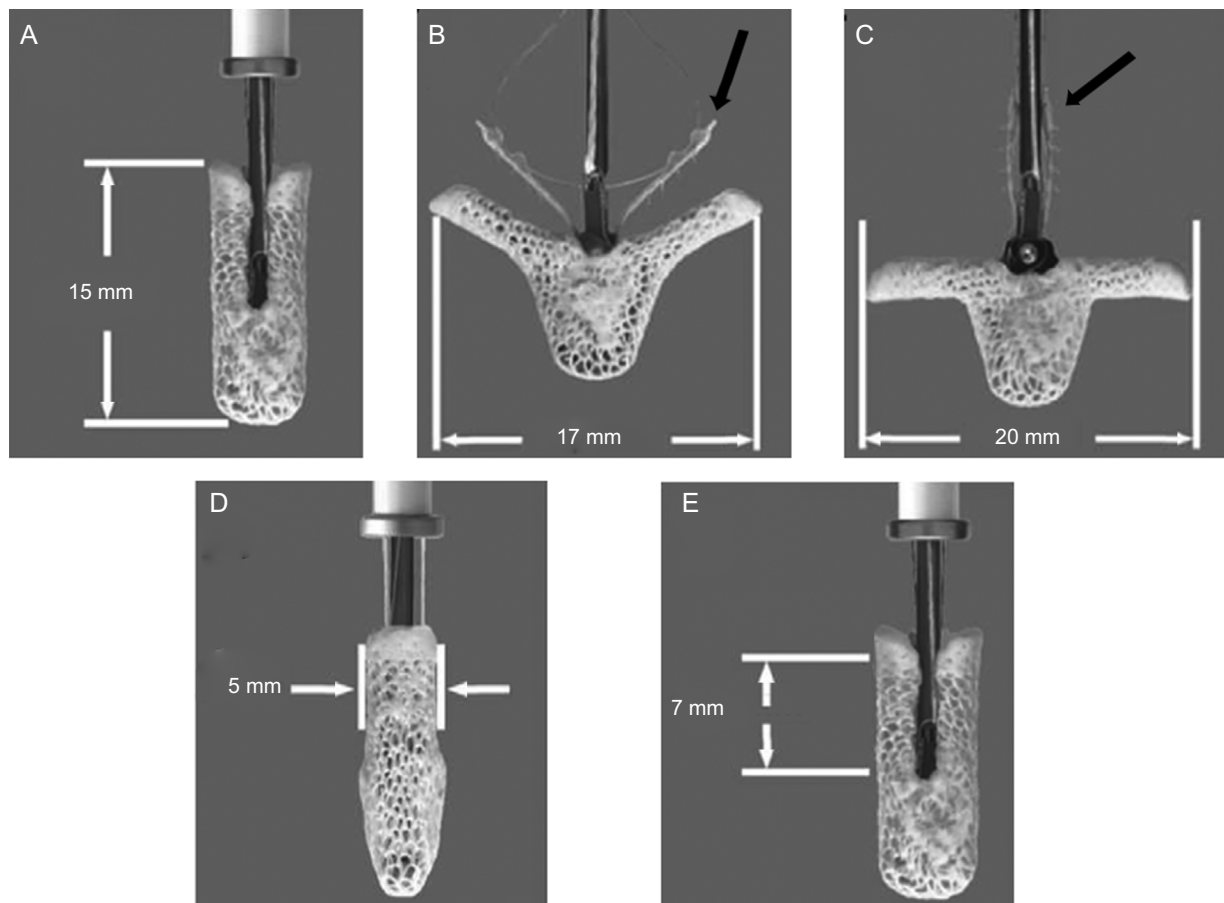


Figure 3. MitraClip System. Clip dimensions and movements. Maximum dimensions of the device: closed (A), open at 120° (B) with the grippers partly closed (black arrow), and open at 180° (C) with grippers totally raised (black arrow). The bottom row shows the maximum leaflet length that can be engaged by the clip arms: 5 mm in width and 7 mm in length. Images edited and reproduced with permission of Abbott Vascular.

steerable guide catheter and a clip delivery system (CDS) that is advanced through the guide. The CDS can be manipulated on all 3 planes. Finally, the MitraClip device is a 5-mm wide chrome-cobalt clip, with 2 articulated arms that can open to 240°. Inside the clip there is a gripper system to firmly grasp the leaflets and create a double mitral orifice. The outer part of the clip is covered in a polyester mesh. The device can be reopened and repositioned, and multiple clips can be implanted to optimize the result^{14,48} (Figure 3).

Contribution of 3-dimensional Visualization to 2-dimensional Mitral Valve Studies

Due to its anatomical complexity, the MV needs to be studied from different views to construct a study system with 2-dimensional TEE that includes 4 midesophageal views and 1 transgastric view.⁴⁹ Using a 3D perspective, and drawing on the experience of MitraClip® implantations, this system can be redefined.

As mentioned above, one of the problems initially faced by pathologists when describing the MV was to define the leaflets, because in fact the MV is a continuous veil-like structure inserted around the mitral annulus, separated by indentations.²² To separate the aortic leaflet from the mural leaflet, pathologists

used the commissures as anatomic markers, which, in turn, were identified by the specific CT type (commissural chordae) that inserted into the commissures, aligned by the PMs²³ In short, the PMs point toward the commissures (Figure 4), and this reference point marks the long axis of the valve, which is the mitral intercommissural view. Following the Carpentier nomenclature,²⁴ the echocardiographic view shows 3 valve scallops, from medial to lateral: P3-A2-P1. When focused on A2-P2, the orthogonal view to the intercommissural view (with the transducer rotated an additional 90°) typically slices the LV outflow tract (LVOT). By slightly rotating the probe manually toward one and then the other commissure, scallops A3-P3 and A1-P1 can be sliced.

The development of matrix-array transducers permits a simultaneous view of 2 orthogonal planes. Using a primary intercommissural view, an orthogonal view along the center shows A2-P2 (Figure 5). If the orthogonal view is rotated laterally toward the lateral scallops, A1-P1 are imaged, and if it is rotated toward the medial segments, A3-P3 are imaged. Finally, to complete the analysis, a 3D view of the valve is obtained (Figure 6). The 3D view improves identification of all the scallops and indentations.

This study protocol, using 3 echocardiographic views (intercommissural, LVOT and 3D), permits an accurate assessment of functional anatomy and the regurgitation site.

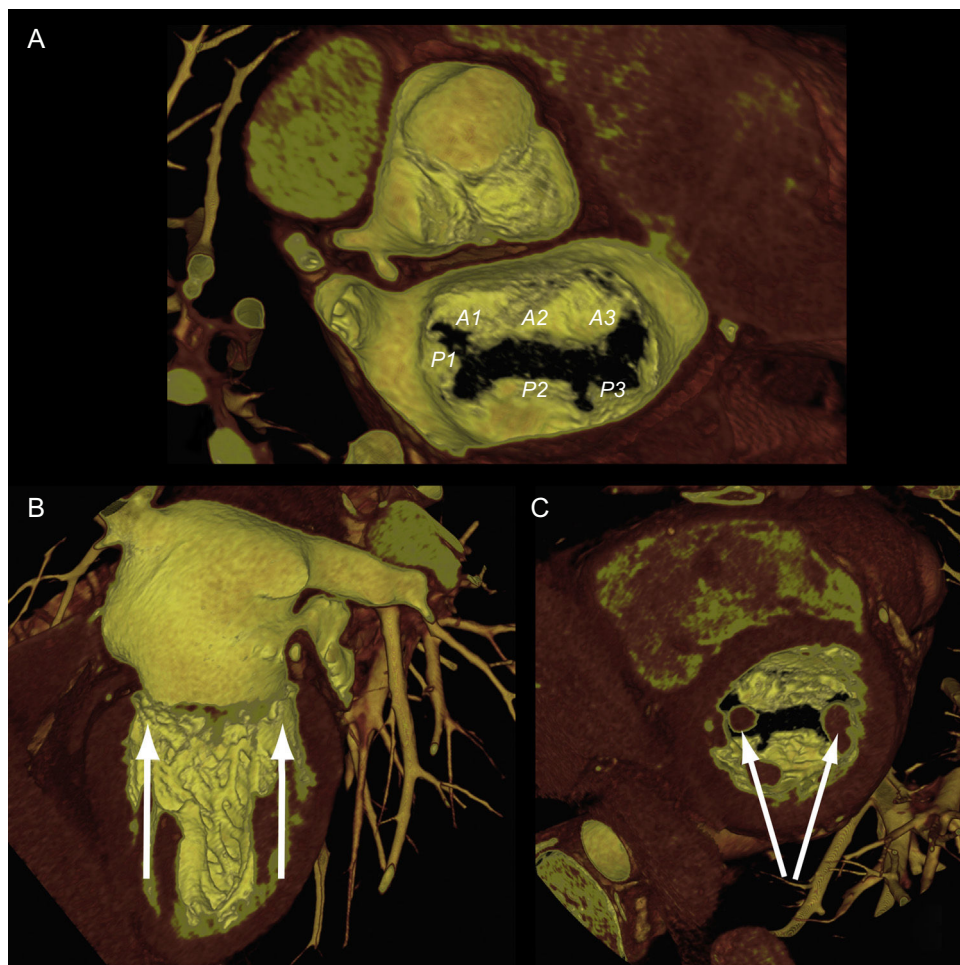


Figure 4. Mitral valve apparatus on cardiac computed tomography. Volume-rendered 3-dimensional reconstruction showing a mitral valve from a surgical view and leaflet scallops identified according to the Carpentier classification (A). Longitudinal (B) and transversal (C) views of the ventricle show the papillary muscles aligned toward the commissural zones.

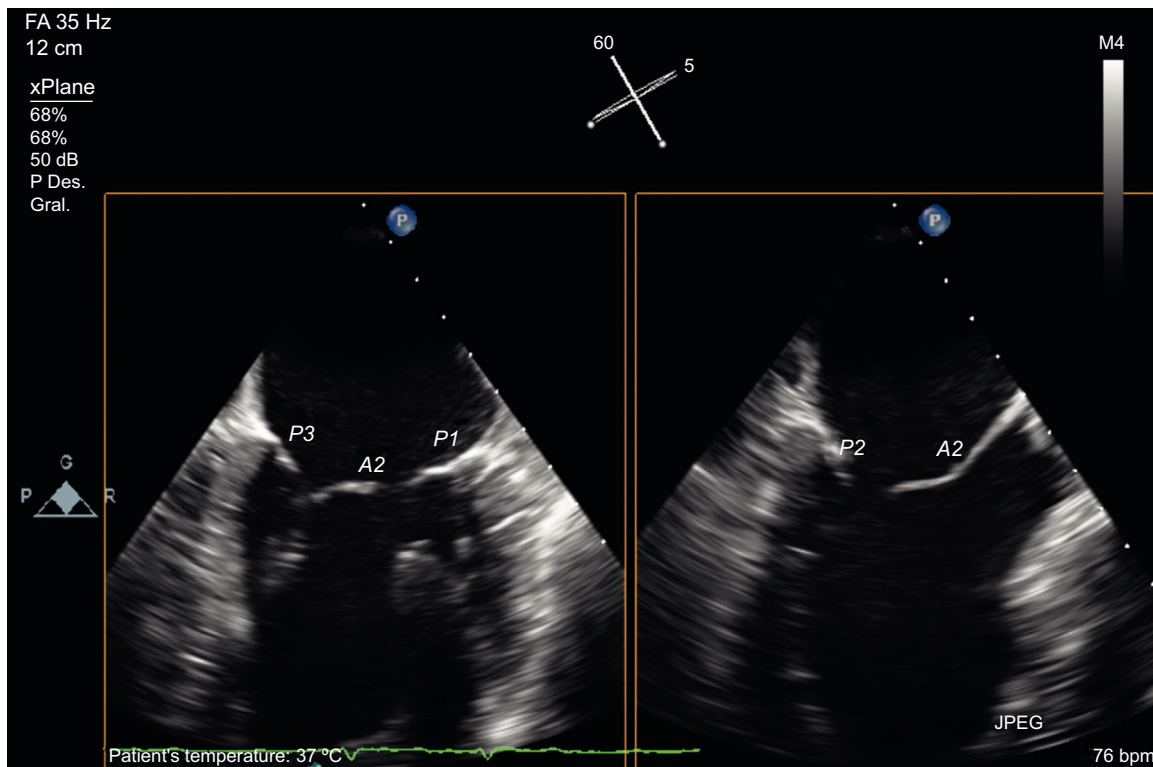


Figure 5. Mitral valve analysis with transesophageal echocardiography. Multiplane transesophageal echocardiography image with simultaneous view of two orthogonal planes. Note the intercommissural view on the left, identified by visualization of 3 independent valve scallops (P3-A2-P1) and the papillary muscle heads. After identifying the long axis of the valve, using the orthogonal view at 90°, the 3-chamber view is found in complete coaxial alignment with the central line of coaptation (A2-P2). The same orthogonal plane is obtained by rotating the plane to 150°.

Patient Selection

The first MV anatomic criteria to select candidates for MV repair with the MitraClip system were established in the EVEREST studies^{48,50,51} (Figure 7). After establishing the safety and feasibility of MitraClip in a phase 1 study,^{48,50} a pilot study was then conducted, called EVEREST II. In this phase 2 study, 279 surgical candidates with MR were randomized in a 2:1 ratio

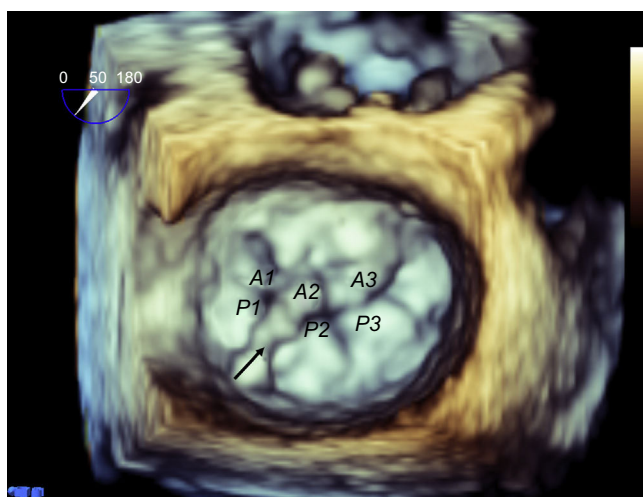


Figure 6. Mitral valve from a surgical view. Three-dimensional transesophageal echocardiography of the mitral valve, providing rapid identification of all valve scallops and detection of a ruptured chord with flail leaflet, affecting scallop A2 alone.

to undergo percutaneous repair or surgery. The patients treated percutaneously had the following clinical profile: 62% were men, mean age was 67 years, 47% had a history of ischemic heart disease (22% of whom had a previous myocardial infarction), 73% had degenerative MR grade III-IV, 91% had symptomatic heart failure, 34% had atrial fibrillation, 40% were in New York Heart Association (NYHA) functional class II, 45% were in NYHA III, and 60% had preserved LV ejection fraction.⁵¹ In real-world practice,^{16,52–55} this clinical profile has shifted toward treatment of patients who are inoperable, older (mean age 71 years), with functional MR (70% of patients), in NYHA III-IV (90%), and preserved ejection fraction (34%). At 9 months of follow-up, these patients were in NYHA I-II (78% of patients), and with MR grade I-II (89%). During the follow-up period, the mortality rate was 15%.⁵⁶

Echocardiographic criteria have also changed. Broader eligibility criteria for MitraClip repair have been applied in view of the positive safety profile of the intervention itself, and the treatment of patients at high surgical risk without other therapeutic options. The successful outcome of the procedure is apparently unaffected by these extended criteria.^{57,58} Current proposed criteria are based on pooled experience, as published by Boekstegers et al,⁵⁹ and detailed in Table 2. Criteria for valve repair are subdivided by valve morphology into 3 categories: EVEREST criteria for optimal valve morphology at centers with limited MitraClip repair experience; acceptable valve morphology, reserved for experienced sites; and difficult or impossible valve morphology.

Implantation Guidance

Echocardiography is an essential technique in MitraClip implantation guidance. At present, these implantations are the interventions that are most dependent on nonfluoroscopic imaging

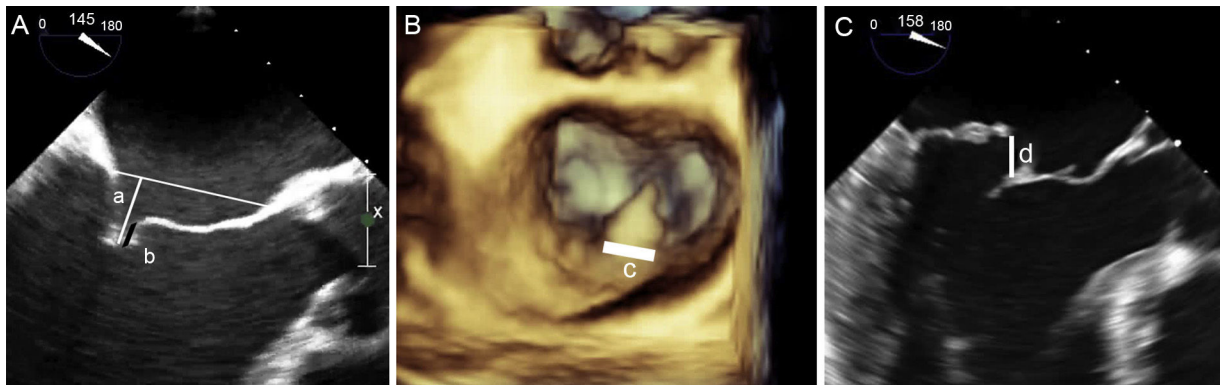


Figure 7. Key anatomic criteria for repairability. A: anatomic criteria for repairability in functional mitral regurgitation; coaptation depth measured from the annulus to the free edge of the leaflets must be < 10 mm (a); coaptation length is the zone of leaflet apposition (b). B and C: key anatomic criteria for repairability in degenerative mitral regurgitation due to prolapse or flail shown through 3-dimensional reconstruction (B) and left ventricular outflow tract plane (C); flail width must be < 15 mm (c) and flail height < 10 mm (d).

guidance. The implantation procedure is summarized in the steps described below.

Transseptal Puncture

This is a critical step in the procedure and the source of most complications. The triaxial catheter system permits 3-directional movements. The transseptal (TS) puncture is the axis from which all movements are made. By aligning the TS site with the central line of mitral coaptation (A2-P2), more precise movements are achieved along the lateral-medial and anterior-posterior axes of the valve. The distance from the TS site to the leaflet coaptation site should be > 40 mm, and ideally about 45 mm, to permit catheter guide maneuvering in the atrium and to advance the CDS into the LV.

An optimal puncture can be achieved usually in the posterior area of the fossa ovalis. To ensure a successful outcome at this initial stage, the echocardiographer must use a common language with the interventional cardiologist:

- The direction in the bicaval view is described as superior-inferior (90°-120°) and it refers to advancing and retracting the TS needle. Superior means cranial movement toward the superior vena cava and inferior refers to caudal movement.
- The direction in the great vessel view is described as anterior-posterior (25°-45°) and refers to TS needle rotation. The

fluoroscopy marker is usually a pigtail catheter in the aorta. Anterior means rotation toward the aorta and posterior means away from the aorta, toward the posterior atrial wall.

The TS imaging guidance protocol includes 3 TEE views: 2 for positioning (bicaval and short axis views) and 1 for height confirmation (4-chamber view at 0°). It is usually recommended to perform the TS puncture as high as possible in the fossa ovalis in the bicaval view and in the mid-posterior zone in the great vessel view, at a height of about 45 mm (Figure 8).

It is generally believed that superior-inferior movement is proportionally reflected in puncture height, ie, if the TS site is at 50 mm, a 5 mm reduction in the bicaval view will lower the TS site to 45 mm. However, this proportionality applies only if the heart is completely vertical, whereas in practice, and especially if there is atrial dilatation, the heart is often in a horizontal position (Figure 9). This is why it may be difficult to locate the puncture site, and cranial-caudal movements may not result in significant changes in height. In these cases, 3D TEE helps clarify catheter behavior and define the puncture site more accurately (Figure 10).

Introduction of the Guide Catheter and Clip Delivery System

After the TS puncture has been performed, the catheters are usually exchanged using an extra-stiff Amplatz® guidewire in the left upper pulmonary vein, under fluoroscopic and ultrasound

Table 2
Extended Anatomic Criteria for MitraClip

Optimal valve morphology	Possible valve morphology	Difficult or impossible valve morphology
Central pathology in scallop 2	Pathology in scallops 1 or 3	Mitral valve perforation or cleft
Absence of valve calcification	Mild calcification outside the grasping zone, annulus calcification, postannuloplasty	Significant calcification in the grasping zone
Mitral valve area > 4 cm ²	Mitral valve area > 3 cm ² with good residual motion	Hemodynamically significant mitral stenosis (MVA < 3 cm ² and mean gradient ≥ 5 mmHg)
Mobile length of posterior leaflet ≥ 10 mm	Mobile length of posterior leaflet 7-10 mm	Mobile length of posterior leaflet < 7 mm
Coaptation depth < 11 mm	Coaptation depth ≥ 11 mm	
Normal leaflet thickness and motion	Restricted motion during systole (Carpentier type IIIb)	Restricted motion during systole and diastole (Carpentier type IIIa)
Flail width < 15 mm and gap < 10 mm	Flail width > 15 mm in case of dilated annulus and possibility of multiple clip implantation	Barlow syndrome with flail in multiple scallops

MVA, mitral valve area.

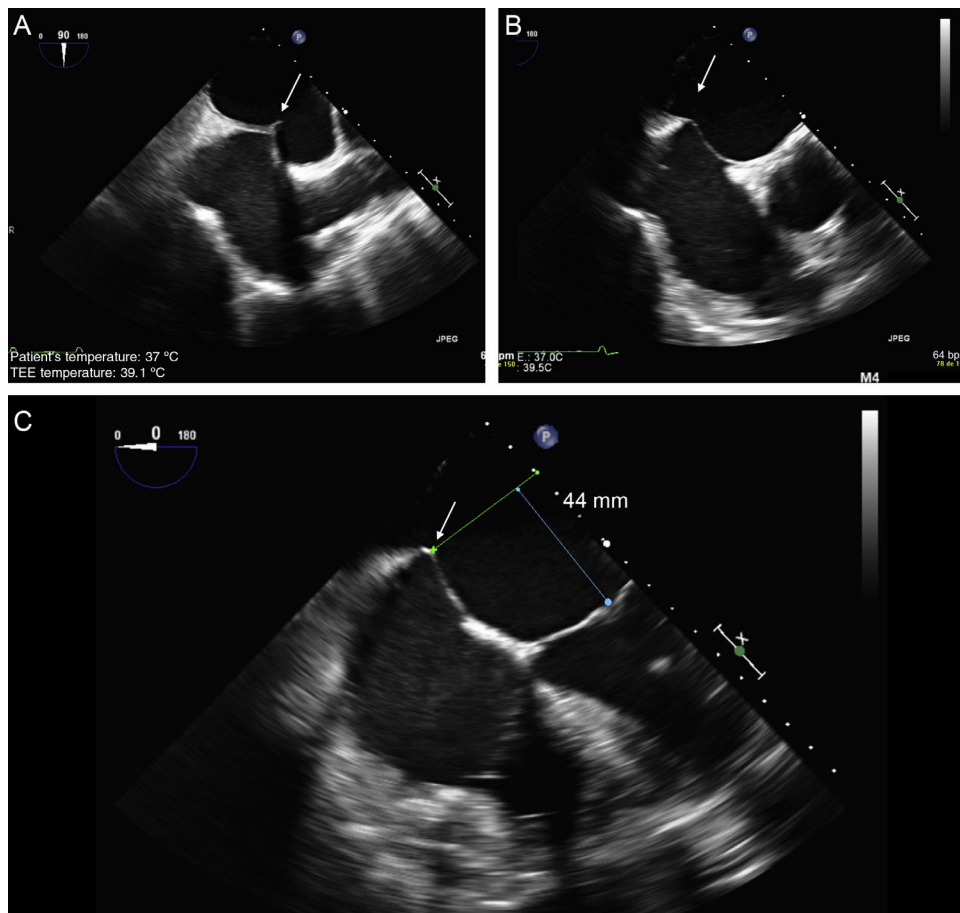


Figure 8. Two-dimensional transesophageal echocardiographic-guided transeptal puncture. A: bicaval view and puncture in the center of the fossa ovalis (arrow). B: short axis view of great vessels with posterior puncture (arrow), away from the aorta. C: 4-chamber plane to measure the height from the puncture site to the valve coaptation line, which should be about 45 mm.

guidance. The steerable guide catheter is advanced, together with a dilator, which can be identified by its tapered tip and echodense markers. The dilator is then withdrawn with the guidewire, and the guide catheter remains in the left atrium. The guide catheter is easily identified by the 2 echodense coils at the tip (Figure 11). The

CDS is then introduced through the guide catheter under ultrasound guidance, avoiding atrial wall damage. The steerable guide catheter and CDS must be positioned using a combination of movements to direct the clip tip to the center of the MV, in the direction of the ventricular apex. The clip path is observed on

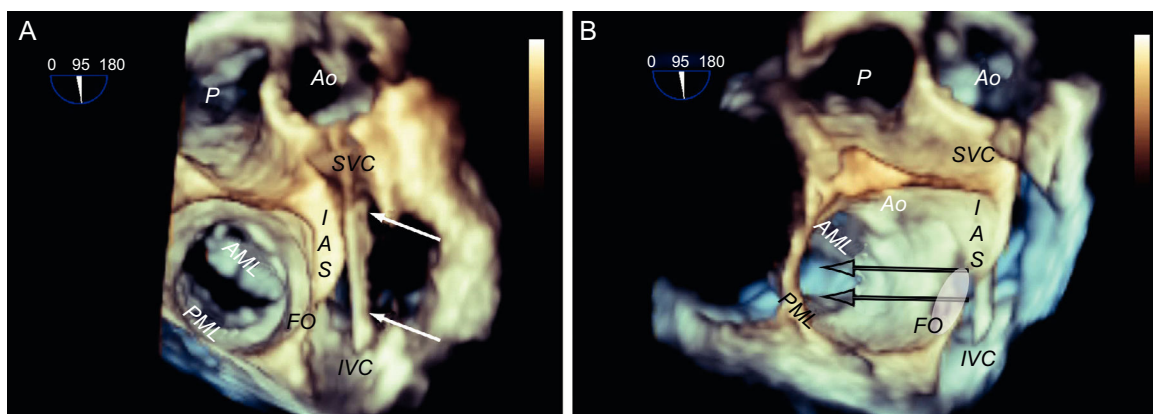


Figure 9. Behavior of the transeptal puncture catheter in horizontal hearts. A: relation between structures and the puncture catheter (arrows); in the cranial position of the interatrial septum, the catheter is located in the anterior region, whereas in the most caudal position, the catheter is located in the posterior region. B: the same image, shown in 3 dimensions and slightly tilted to show the relation between the fossa ovalis and the mitral coaptation line; note that the cranial-caudal catheter trajectory has little impact on the puncture height (arrows), which depends more on the anterior-posterior position; when the catheter turns toward the aorta, the puncture site is lower, and when it turns away from the aorta, the puncture site is higher. AML, anterior mitral leaflet; Ao, aorta; FO, fossa ovalis; IAS, interatrial septum; IVC, inferior vena cava; PML, posterior mitral leaflet; SVC, superior vena cava.

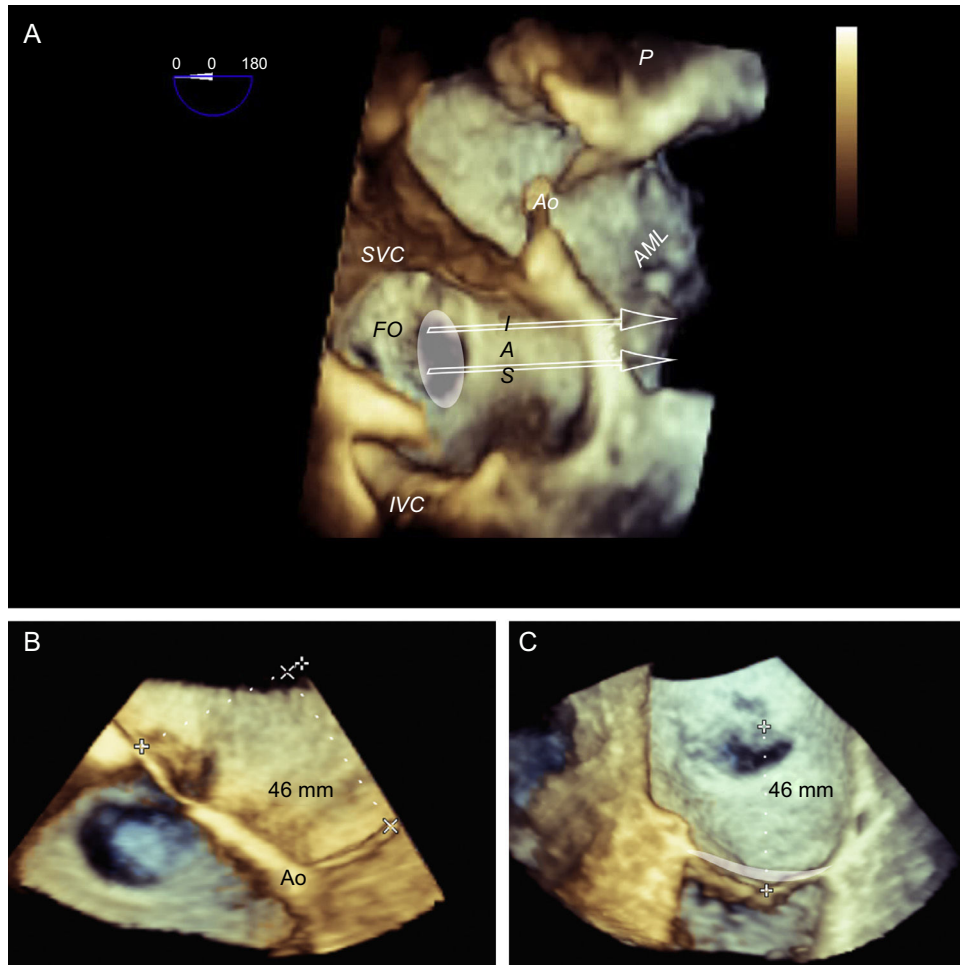


Figure 10. Preprocedural 3-dimensional planning of the transeptal puncture. Image of 3-dimensional transesophageal echocardiography from a ventricular view (A), showing the horizontal heart position and how cranial-caudal catheter movements have little impact on the puncture height above the mitral coaptation line (arrows); therefore, a central puncture can be performed with a bicaval view without affecting height. B: 3-dimensional 4-chamber view; puncture in the most posterior zone of the fossa (away from the aorta) measures about 45 mm in height. C: modified 3-dimensional view with the interatrial septum *en face*, aligning the mitral annulus to the Z plane; this movement permits more accurate measurements, such that the height from the posterior zone of the fossa to the coaptation line is 46 mm. Combining the data from the 3 images, transeptal puncture can be planned at the center of the fossa ovalis in the bicaval view and in the posterior zone in the great vessel view. This location differs slightly from the superior, posterior puncture that is usually recommended. AML, anterior mitral leaflet; Ao, aorta; FO, fossa ovalis; IAS, interatrial septum; IVC, inferior vena cava; SVC, superior vena cava.

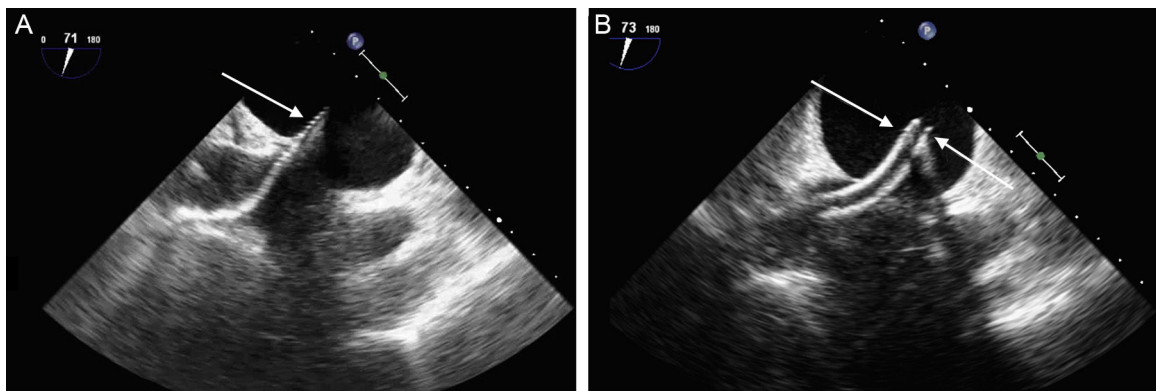


Figure 11. Transeptal access monitoring. A: transesophageal echocardiographic image showing the dilator crossing the interatrial septum, with echodense markers at the tip (arrow). B: image of the guide catheter after withdrawal of the dilator. Markers denote the guide catheter tip (arrows).

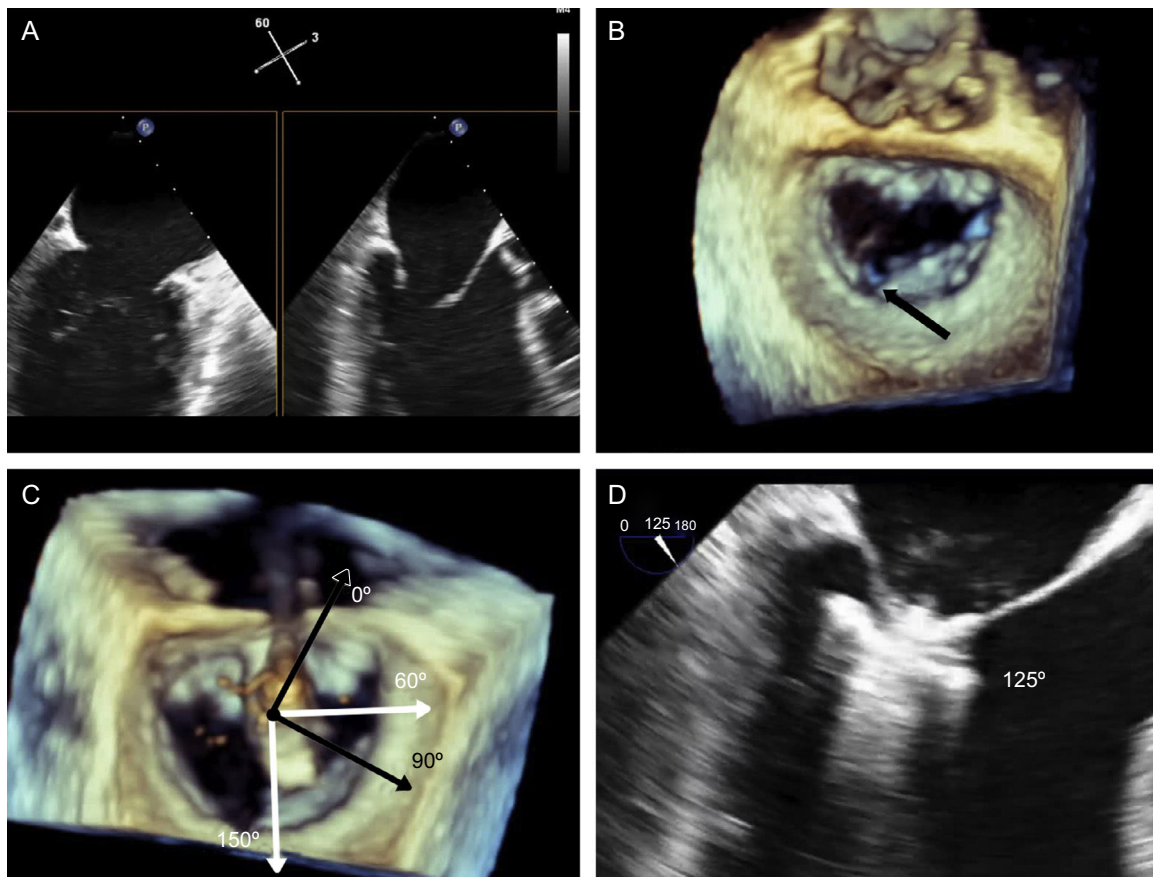


Figure 12. Implantation plane. The geometry of this mitral valve shows the intercommissural view at 60° (A), and therefore the left ventricular outflow tract is at 150°. However, due to the marked indentation separating P1 from P2 (B, arrow), the implantation plane is slightly angulated. To locate the implantation plane, 3-dimensional transesophageal echocardiography must be used to first confirm coaxial alignment with the target zone (C); then the 2-dimensional view must be sought by moving the transducer, to achieve the best view of both open arms (D).

echocardiography, usually via a view with orthogonal intercommissural and LVOT planes.

The next step is to align the clip arms with the valve coaptation line by rotating them clockwise and counterclockwise until coaxial alignment is achieved. Three-dimensional TEE and a surgical view are used to position the MV with the aorta at 12 o'clock and the left atrial appendage at 9 o'clock (Figure 12).

Clip Delivery System Advance and Leaflet Grasping

After checking that the CDS is perpendicular and the clip is aligned coaxially, the system is advanced into the LV. These steps are essential to minimize clip movement in the LV and avoid complications with the CT. In the case of a first clip, the CDS is advanced with the arms open and pointing, usually, toward the center of the regurgitant jet. These steps are monitored with simultaneous orthogonal intercommissural and LVOT planes. It is important to select the best TEE plane for clip deployment monitoring, in the same way that the best fluoroscopic view should be selected in percutaneous aortic device implantation.⁶⁰ The best plane varies according to the individual patient. If the center of A2-P2 is the planned target site for clip deployment, selecting a good intercommissural plane permits the clip plane to be defined by adding 90° to the intercommissural plane. If the planned target site is elsewhere, after confirming that the system is in coaxial alignment with the valve on 3D TEE, the transesophageal probe and transducer must be positioned around the LVOT plane to provide the best full view of the clip (Figure 12).

Once the clip is inside the ventricle, the main focus is on grasping the leaflets. This process is monitored via an extended view of the implantation plane. Leaflet engagement is achieved by retracting the clip with the arms open, and maneuvering the catheter until the leaflets rest on the arms (Figure 12). When a grasp is obtained, the grippers are lowered, the clip arms are closed and valve function is assessed.

Valve Function Assessment

Assessment of the grasping effect is a key aspect that depends entirely on echocardiography. The assessment covers 3 aspects: reduction of regurgitant jet, degree of stenosis generated, and grasping anatomy.

Residual regurgitation must be assessed under the hemodynamic conditions (blood pressure, vasoactive support) and technical conditions (echographic parameters) that most closely mimic the baseline regurgitation assessment in the catheterization laboratory and under general anesthesia. European and American echocardiography societies have published guidelines on the different criteria for grading MR severity.^{3,61} While it is beyond the scope of this article to provide an exhaustive analysis of MR grading, we will, however, comment on the limitations of some assessment methods following MitraClip deployment. There is no agreement on how to evaluate residual MR after creation of a double or triple mitral orifice.⁶² Although a central echocardiographic laboratory analysis found significant changes in regurgitant volume, color flow Doppler, and pulmonary vein flow,⁶³ a

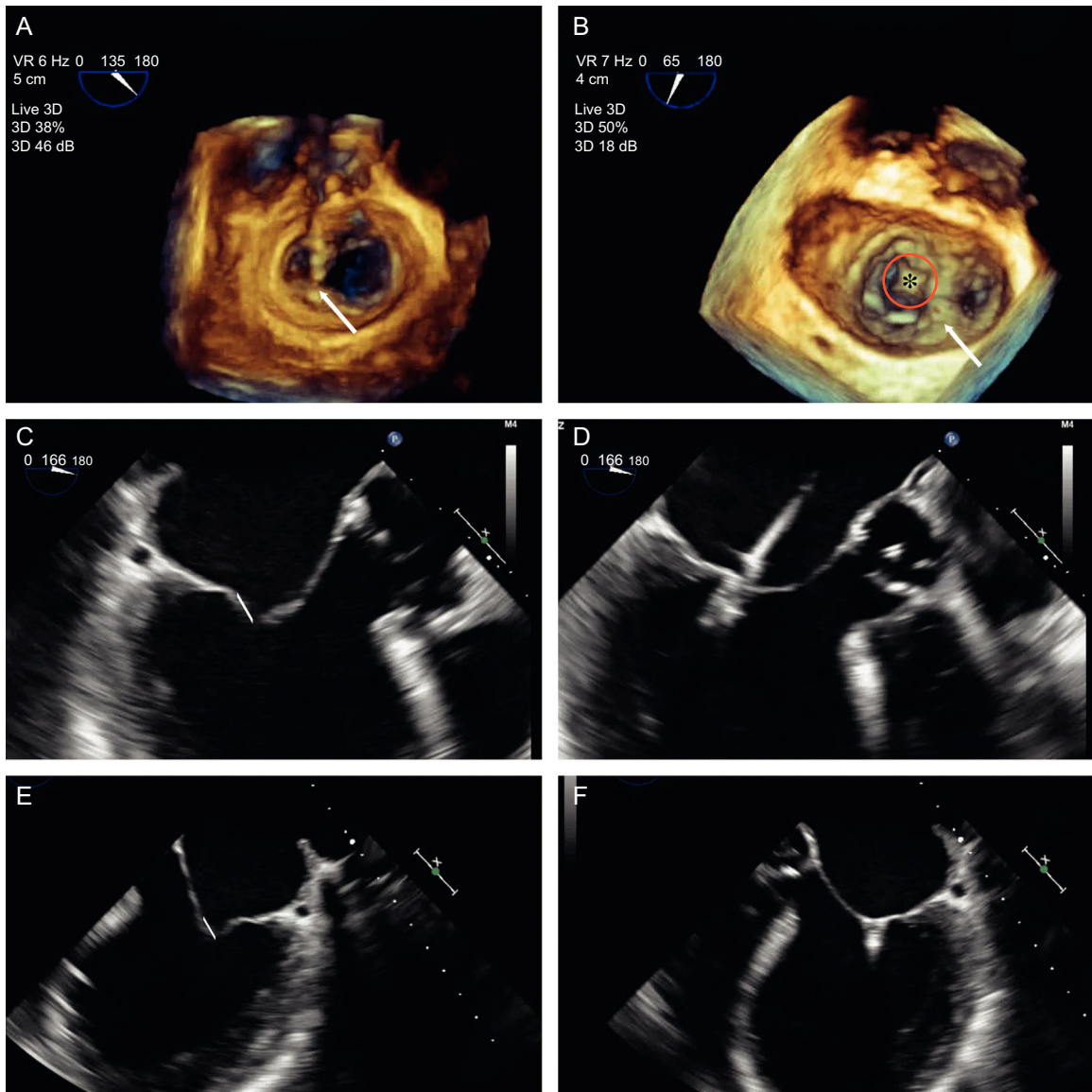


Figure 13. Grasping anatomy. The extent of grasping can be analyzed with 3-dimensional transesophageal echocardiography of the mitral valve. A: extent of posterior leaflet insertion is less than the width of the clip (arrow), with an image of the narrow “pyramid” vertex. B: the clip has detached from the posterior leaflet (asterisk) and a new clip has been deployed medially to the first clip; note the width of the “pyramid” vertex from the new clip (arrow) compared with the first. C-E: length of posterior (C and D) and anterior (E and F) leaflets engaged by the clip, obtained by small panning movements with the probe around the clip.

recent study has shown poor interobserver agreement and overestimation of residual MR grading by TEE compared with cardiac MRI.⁶⁴

A multiparametric approach should therefore be used, similar to the approach for native valve assessment,^{3,61} and taking into account some specific aspects:

- Color Doppler jet area assessment overestimates regurgitation grade when multiple jets are involved.⁶⁵
- Mitral E-wave velocity increases in parallel with increased valve stenosis.^{3,61,66}
- Quantitation using the Proximal Isovelocity Surface Area (PISA) method is not validated in the presence of more than 1 regurgitant orifice.⁶⁷
- The additive measurement of venas contractas is not validated in the presence of more than 1 regurgitant orifice.
- A significant reduction in MR grade is reflected in an immediate hemodynamic change, which can be confirmed by lack of

pulmonary vein systolic flow wave reversal, normalized left atrial pressure, increased cardiac output and systolic arterial pressure, and reduced vascular resistance.⁶⁸

Significant valve stenosis (defined as a mitral valve orifice area $< 1.5 \text{ cm}^2$) is extremely rare when 1 to 2 clips are implanted, and there is no evidence of progression at 4 years of follow-up.^{48,69} A faster and more feasible alternative is to perform a mean gradient assessment in the catheterization laboratory. A 5 mmHg cut-off predicts an elevated gradient at discharge.⁷⁰

After achieving a satisfactory reduction in MR with the clip, a protocol should be applied to evaluate the anatomy of the tissue surrounding the clip, to reduce the chance of detachment.^{44,71} This protocol includes an assessment of anterior leaflet motion and interrogation of leaflet insertion in a 0° view, posterior leaflet motion and interrogation of leaflet insertion in the implantation view (usually the LVOT view), and extent of insertion of both leaflets using 3D imaging (Figure 13):

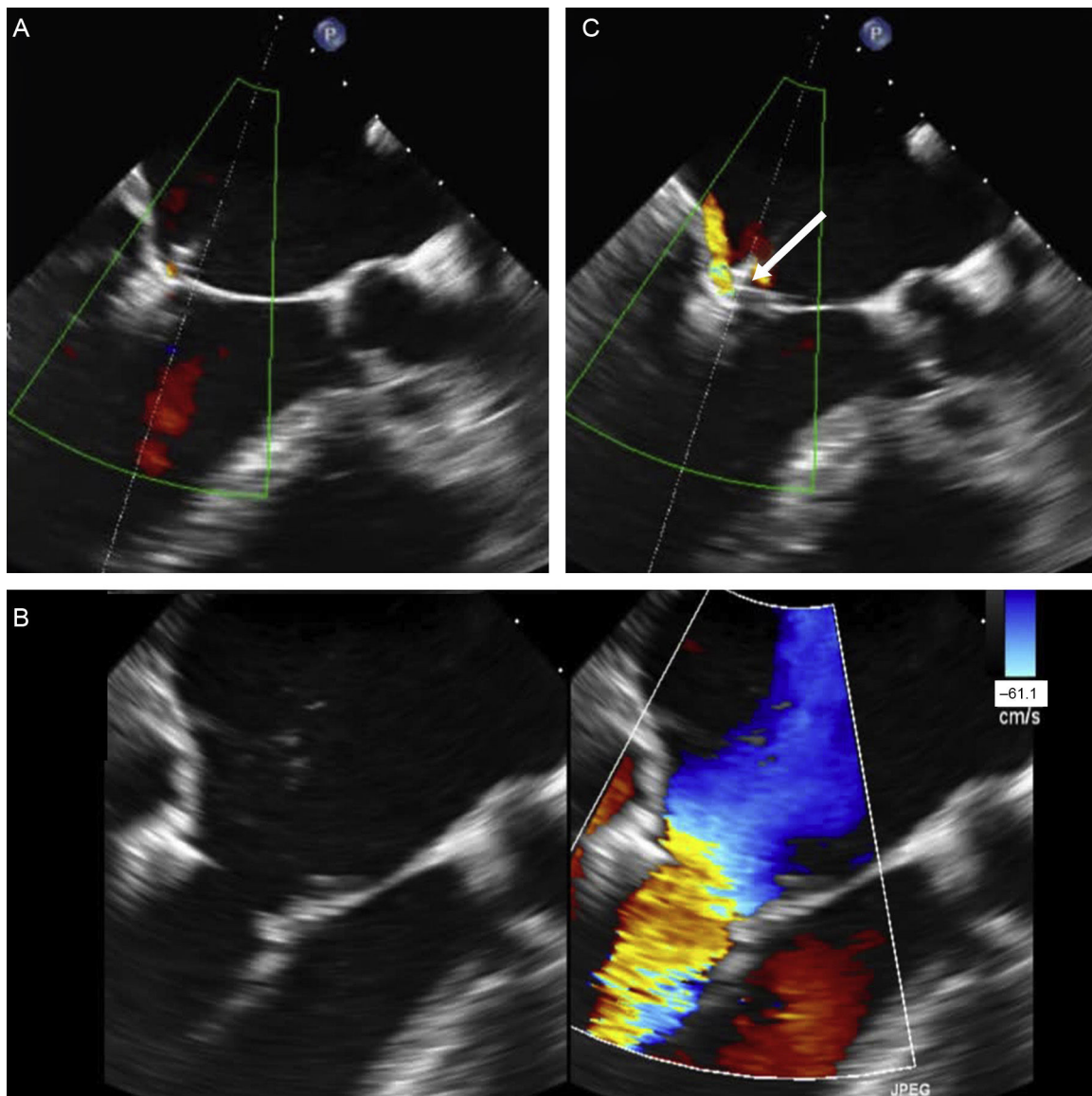


Figure 14. Acute detachment of the anterior leaflet. A: both leaflets appear to have engaged well, with reduced leaflet motion. B: however, acute detachment of the anterior leaflet is observed after clip release. C: careful observation of leaflet engagement shows a moving structure above the clip (arrow), and a regurgitant jet that originates here. Implantation of a first clip hinders the grasping analysis of a second clip.

- The 0° and LVOT views should show restricted motion of the anterior and posterior leaflets, respectively. The length of inserted leaflet can be measured by slightly rotating the probe manually. The recommended length is ≥ 5 mm, although it may measure up to 7 mm.
- A 3D image should show the extent of inserted tissue and formation of 2 pyramids with vertices measuring at least 5 mm, which is the width of the clip. If a large quantity of tissue is engaged in the clip, the pyramid vertices will be wider than the clip itself, probably due to the tension generated.

Device Deployment

If valve function is deemed satisfactory, the device can be deployed. If it is unsatisfactory, the device can be repositioned. This step should be performed under ultrasound guidance to detect any complications. Increased regurgitant jet is the most common

complication, although it has not been reported in the literature. Clip deployment eliminates the support from the CDS and accumulated tension. This changes the relationship of the device with adjacent valve tissue and increases the regurgitant jets on both sides of the clip, due to newly-created commissures.

Detachment from a single leaflet is a much-feared but rare complication (Figure 14). Complete clip detachment with embolization has not been reported. Implementation of an implantation analysis protocol has reduced the incidence of single leaflet detachment from 14.3%⁴⁷ in animal experimentation and 4.8%⁵² at the start of clinical experience to a current figure of 1.9%.⁵³

PREPROCEDURAL COMPUTED TOMOGRAPHY IN PERCUTANEOUS REPAIR FOR MITRAL REGURGITATION

Several factors favor the use of cardiac CT when planning a percutaneous repair for MR, and more specifically, transcatheter mitral valve implantation. There are significant differences

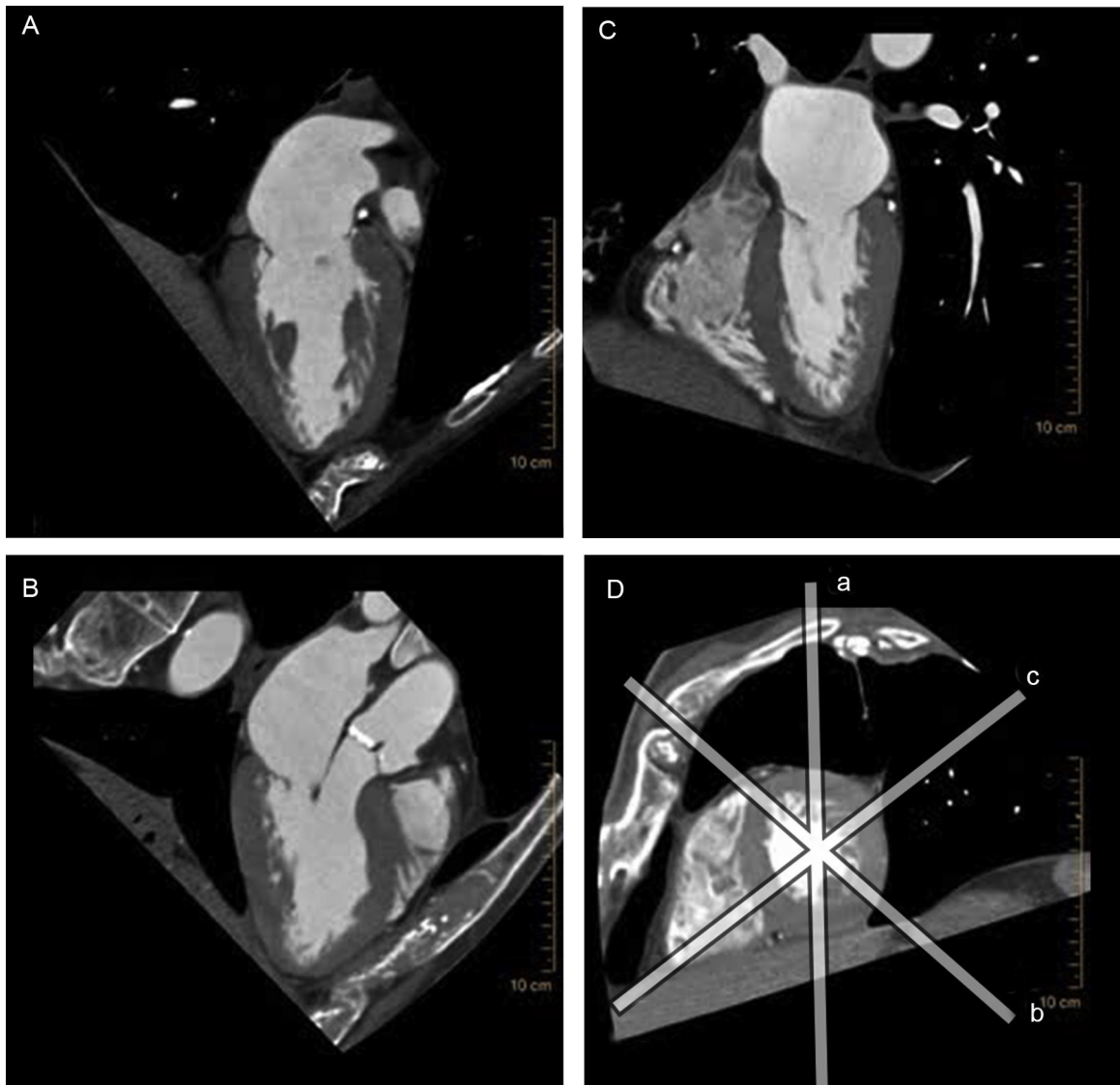


Figure 15. Multiplane reconstruction in cardiac computed tomography. Note the excellent spatial resolution on all 3 planes, permitting a detailed analysis of the entire mitral valve apparatus. A: vertical longitudinal plane of the heart. B: 3-chamber plane with the left ventricular outflow tract. C: horizontal longitudinal plane of the heart. D: short axis of the heart, sliced by the other 3 planes (a-c).

between the mitral and aortic valves when planning transcatheter valve implantations: the mitral valve is somewhat calcified, the annulus is larger and has a 3D saddle shape, the subvalvular apparatus is complex, and the LV outflow tract needs to be preserved (Figure 15). This complex anatomy warrants the use of 3D imaging techniques for preprocedural studies,⁷² and, at present, cardiac CT offers the highest 3D spatial resolution of all techniques.

Cardiac CT contributes to transcatheter mitral valve implantation planning in different ways, depending on the implantation site. The Fortis device (Edwards Lifesciences; Irvine, California, United States) is implanted via a transapical approach and is anchored directly on the anterior and posterior leaflets. At the planning stage of this intervention, computed tomography is an adjunct to echocardiography in annulus and leaflet evaluation, and is proving essential in subvalvular apparatus evaluation. Complicated subvalvular anatomy can hinder system advance and device anchoring due to irregular PM branching or fusion, or the presence of prolonged struts or CTs that insert beyond the rough zone of the leaflets.^{73,74} The Tiara (Neovasc Inc.; Richmond, Canada)

transapical mitral prosthesis rests on the atrial surface of the mitral annulus and is anchored on the ventricular surface beside the fibrous trigones and posterior annulus (Figure 16). Cardiac CT has been used for Tiara implantation to achieve a more accurate measurement of the annulus and to plan the best fluoroscopic angulation.^{41,75,76}

Blanke et al⁷⁷ published an article with the aim of standardizing the terms that are starting to appear in mitral valve apparatus geometry, and to assess the different imaging techniques used in the planning, intervention, and follow up of transcatheter mitral valve implantation.

Cardiac CT has also been used to plan percutaneous coronary sinus-based indirect annuloplasty for MR, with implantation of the CARILLON system. One of the complications that prevents device implantation is coronary circumflex artery compression. Despite the excellent spatial resolution of cardiac CT in the analysis of coronary venous anatomy⁷⁸ and adjacent structures, procedural success in the AMADEUS trial⁷⁹ remained unchanged with advance knowledge of this anatomy.

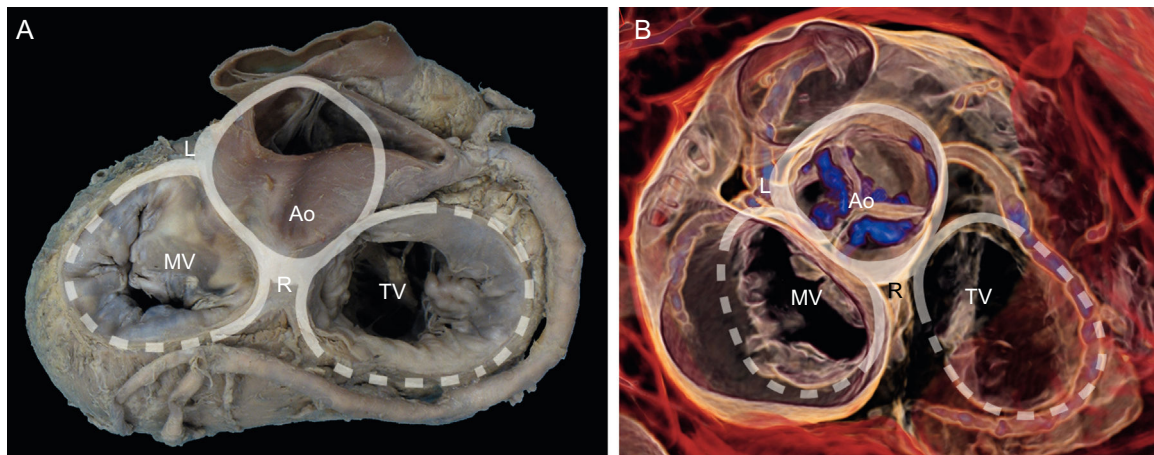


Figure 16. Volume-rendered 3-dimensional cardiac computed tomography. Note the relation of the anatomic structures around the fibrous skeleton for preprocedural planning of transcatheter valve implantation. Ao, aorta; L, left fibrous trigone; MV, mitral valve; R, right fibrous trigone; TV, tricuspid valve.

CONCLUSIONS

Percutaneous repair for MR in native valves is an emerging intervention that relies heavily on other imaging techniques beyond fluoroscopy. At present, the main technique for patient selection and intervention guidance is 3D TEE. The technical complexity of percutaneous repair makes specific training in this field absolutely essential for interventional cardiologists and cardiac imaging specialists alike. Additional training in advanced cardiac imaging techniques such as cardiac CT and cardiac MRI is also necessary.

Cardiac CT provides accuracy, reproducibility and a wide field of view in transcatheter aortic valve interventions and similarly in MV repair, by permitting a 3D analysis of the heart and adjacent structures. Considering the complexity of MV anatomy, cardiac CT provides valuable additional information to the restricted field of view of echocardiography, making this technique determinant in the planning and guidance of some percutaneous procedures.

The potential for cardiac MRI lies in the absence of ionizing radiation and its versatility, offering a comprehensive study of anatomy, function, blood flow and tissue characterization. Future improvements in cardiac MRI availability, data acquisition times, and spatial resolution will play a key role in making this technique a strong contender in the field of imaging techniques for percutaneous interventions.

ACKNOWLEDGEMENTS

We are grateful to Prof. Alfonso Rodríguez Baeza, Professor of the Department of Morphologic Sciences at the Faculty of Medicine of the UAB (*Universitat Autònoma de Barcelona*), for answering our questions and for providing the anatomy images published in this article, and to Jorge Carbajo and María Perez at Abbott Vascular, for their assistance and advice in technical aspects. We would also particularly like to thank Nuria López and Martina Li for their patience and support.

CONFLICTS OF INTEREST

C.H. Li and D. Arzamendi are advisers for Abbott and have received nonspecific support for conducting various research projects.

REFERENCES

- Nkomo VT, Gardin JM, Skelton TN, Gottdiener JS, Scott CG, Enriquez-Sarano M. Burden of valvular heart diseases: a population-based study. *Lancet*. 2006;368:1005–11.
- lung B, Baron G, Butchart EG, Delahaye F, Gohlke-Bärwolf C, Levang OW, et al. A prospective survey of patients with valvular heart disease in Europe: The Euro Heart Survey on Valvular Heart Disease. *Eur Heart J*. 2003;24:1231–43.
- Vahanian A, Alfieri O, Andreotti F, Antunes MJ, Barón-Esquivias G, Baumgartner H, et al. Guidelines on the management of valvular heart disease (version 2012). *Eur Heart J*. 2012;33:2451–96.
- Madu EC, D’Cruz IA. The vital role of papillary muscles in mitral and ventricular function: echocardiographic insights. *Clin Cardiol*. 1997;20:93–8.
- Ling LH, Enriquez-Sarano M, Seward JB, Tajik AJ, Schaff HV, Bailey KR, et al. Clinical outcome of mitral regurgitation due to flail leaflet. *N Engl J Med*. 1996;335:1417–23.
- Avierinos JF, Gersh BJ, Melton LJ, Bailey KR, Shub C, Nishimura RA, et al. Natural history of asymptomatic mitral valve prolapse in the community. *Circulation*. 2002;106:1355–61.
- Rosenhek R, Rader F, Klaar U, Gabriel H, Krejc M, Kalbeck D, et al. Outcome of watchful waiting in asymptomatic severe mitral regurgitation. *Circulation*. 2006;113:2238–44.
- Tribouilloy C, Grigioni F, Avierinos JF, Barbieri A, Rusinaru D, Szymanski C, et al. Survival implication of left ventricular end-systolic diameter in mitral regurgitation due to flail leaflets. A long-term follow-up multicenter study. *J Am Coll Cardiol*. 2009;54:1961–8.
- Mirabel M, lung B, Baron G, Messika-Zeitoun D, Détaint D, Vanoverschelde JL, et al. What are the characteristics of patients with severe, symptomatic, mitral regurgitation who are denied surgery? *Eur Heart J*. 2007;28:1358–65.
- Grigioni F, Tribouilloy C, Avierinos JF, Barbieri A, Ferlito M, Trojette F, et al. Outcomes in mitral regurgitation due to flail leaflets. A multicenter European study. *JACC Cardiovasc Imaging*. 2008;1:133–41.
- Mihaljevic T, Lam BK, Rajeswaran J, Takagaki M, Lauer MS, Gillinov AM, et al. Impact of mitral valve annuloplasty combined with revascularization in patients with functional ischemic mitral regurgitation. *J Am Coll Cardiol*. 2007;49:2191–201.
- Whitlow PL, Feldman T, Pedersen WR, Lim DS, Kipperman R, Smalling R, et al. Acute and 12-month results with catheter-based mitral valve leaflet repair: the EVEREST II (Endovascular Valve Edge-to-Edge Repair) High Risk Study. *J Am Coll Cardiol*. 2012;59:130–9.
- Chiam PTL, Ruiz CE. Percutaneous transcatheter mitral valve repair. *JACC Cardiovasc Interv*. 2011;4:1–13.
- Nombela-Franco L, Urena M, Barbosa Ribeiro H, Rodés-Cabau J. Avances en el tratamiento percutáneo de la insuficiencia mitral. *Rev Esp Cardiol*. 2013;66:566–82.
- Ruiz CE, Klinger C, Perk G, Maisano F, Cabalka AK, Landzberg M, et al. Transcatheter therapies for the treatment of valvular and paravalvular regurgitation in acquired and congenital valvular heart disease. *J Am Coll Cardiol*. 2015;66:169–83.
- Carrasco-Chinchilla F, Arzamendi D, Romero M, Gimeno de Carlos F, Alonso-Briales JH, Li CH, et al. Experiencia inicial del tratamiento percutáneo de la regurgitación mitral con dispositivo MitraClip® en España. *Rev Esp Cardiol*. 2014;67:1007–12.
- Levine RA, Triulzi MO, Harrigan P, Weyman AE. The relationship of mitral annular shape to the diagnosis of mitral valve prolapse. *Circulation*. 1987;75:756–67.

18. Levine RA, Handschumacher MD, Sanfilippo AJ, Hagege AA, Harrigan P, Marshall JE, et al. Three-dimensional echocardiographic reconstruction of the mitral valve, with implications for the diagnosis of mitral valve prolapse. *Circulation*. 1989;80:589–98.
19. Kopuz C, Erk K, Sancar Baris Y, Onderoglu S, Sinav A. Morphometry of the fibrous ring of the mitral valve. *Ann Anat*. 1995;177:151–4.
20. Angelini A, Ho SY, Anderson RH, Davies MJ, Becker AE. A histological study of the atrioventricular junction in hearts with normal and prolapsed leaflets of the mitral valve. *Br Heart J*. 1988;59:712–6.
21. Berdajs D, Zünd G, Camenisch C, Schurr U, Turina MI, Genoni M. Annulus fibrosus of the mitral valve: reality or myth. *J Card Surg*. 2007;22:406–9.
22. Ranganathan N, Lam JH, Wigle ED, Silver MD. Morphology of the human mitral valve. II. The valve leaflets. *Circulation*. 1970;41:459–67.
23. Edwards JE, Rusted IE, Scheffley CH. Studies of the mitral valve. II. Certain anatomic features of the mitral valve and associated structures in mitral stenosis. *Circulation*. 1956;14:398–406.
24. Carpentier AF, Lessana A, Relland JY, Belli E, Mihaileanu S, Berrebi AJ, et al. The "physio-ring": an advanced concept in mitral valve annuloplasty. *Ann Thoracic Surg*. 1995;60:1177–86. discussion 1185–6.
25. Grande-Allen KJ, Clabro A, Gupta V, Wight TN, Hascall VC, Vesely I. Glycosaminoglycans and proteoglycans in normal mitral valve leaflets and chordae: association with regions of tensile and compressive loading. *Glycobiology*. 2004;14:621–33.
26. Lam JH, Ranganathan N, Wigle ED, Silver MD. Morphology of the human mitral valve. I. Chordae tendineae: a new classification. *Circulation*. 1970;41:449–58.
27. Castillo JG, Solís J, González-Pinto A, Adams DH. Ecocardiografía quirúrgica de la válvula mitral. *Rev Esp Cardiol*. 2011;64:1169–81.
28. Carpentier A. Cardiac valve surgery—the "French correction". *J Thorac Cardiovasc Surg*. 1983;86:323–37.
29. Chen JJ, Manning MA, Frazier AA, Judy J, White CS. CT angiography of the cardiac valves: normal, diseased, and postoperative appearances. *Radiographics*. 2009;29:1393–412.
30. Kisslo J, Firek B, Ota T, Kang DH, Fleishman CE, Stetten G, et al. Real-time volumetric echocardiography: the technology and the possibilities. *Echocardiography*. 2000;17:773–9.
31. Wang XF, Deng YB, Nanda NC, Deng J, Miller AP, Xie MX. Live three-dimensional echocardiography: imaging principles and clinical application. *Echocardiography*. 2003;20:593–604.
32. Scheffler K, Lehnhardt S. Principles and applications of balanced SSFP techniques. *Eur Radiol*. 2003;13:2409–18.
33. Pooley RA. AAPM/RSNA physics tutorial for residents: fundamental physics of MR imaging. *Radiographics*. 2005;25:1087–99.
34. Bitar R, Leung G, Perng R, Tadros S, Moody AR, Sarrazin J, et al. MR pulse sequences: what every radiologist wants to know but is afraid to ask. *Radiographics*. 2006;26:513–37.
35. Cody DD, Mahesh M. AAPM/RSNA physics tutorial for residents: Technologic advances in multidetector CT with a focus on cardiac imaging. *Radiographics*. 2007;27:1829–37.
36. Dalrymple NC, Prasad SR, Freckleton MW, Chintapalli KN. Informatics in radiology (infoRAD): introduction to the language of three-dimensional imaging with multidetector CT. *Radiographics*. 2005;25:1409–28.
37. Schueler BA. The AAPM/RSNA physics tutorial for residents: general overview of fluoroscopic imaging. *Radiographics*. 2000;20:1115–26.
38. Morris MF, Maleszewski JJ, Suri RM, Burkhardt HM, Foley TA, Bonnicksen CR, et al. CT and MR imaging of the mitral valve: radiologic-pathologic correlation. *Radiographics*. 2010;30:1603–20.
39. Blanke P, Dvir D, Cheung A, Ye J, Levine RA, Precious B, et al. A simplified D-shaped model of the mitral annulus to facilitate CT-based sizing before transcatheter mitral valve implantation. *J Cardiovasc Comput Tomogr*. 2014;8:459–67.
40. Blanke P, Dvir D, Cheung A, Levine RA, Thompson C, Webb JG, et al. Mitral annular evaluation with CT in the context of transcatheter mitral valve replacement. *JACC Cardiovasc Imaging*. 2015;8:612–5.
41. Blanke P, Dvir D, Naoum C, Cheung A, Ye J, Thériault-Lauzier P, et al. Prediction of fluoroscopic angulation and coronary sinus location by CT in the context of transcatheter mitral valve implantation. *J Cardiovasc Comput Tomogr*. 2015;9:183–92.
42. Maisano F, Torracca L, Oppizzi M, Stefano PL, D'Addario G, La Canna G, et al. The edge-to-edge technique: a simplified method to correct mitral insufficiency. *Eur J Cardiothorac Surg*. 1998;13:240–6.
43. Alfieri O, Maisano F, De Bonis M, Stefano PL, Torracca L, Oppizzi M, et al. The double-orifice technique in mitral valve repair: a simple solution for complex problems. *J Thorac Cardiovasc Surg*. 2001;122:674–81.
44. Maisano F, La Canna G, Colombo A, Alfieri O. The evolution from surgery to percutaneous mitral valve interventions: the role of the edge-to-edge technique. *J Am Coll Cardiol*. 2011;58:2174–82.
45. Nifong LW, Chu VF, Bailey BM, Maziarz DM, Sorrell VL, Holbert D, et al. Robotic mitral valve repair: experience with the da Vinci system. *Ann Thorac Surg*. 2003;75:438–42. discussion 443.
46. Webb JG, Maisano F, Vahanian A, Munt B, Naqvi TZ, Bonan R, et al. Percutaneous suture edge-to-edge repair of the mitral valve. *EuroIntervention*. 2009;5:86–9.
47. St. Goar FG, Fann JJ, Komtebedde J, Foster E, Oz MC, Fogarty TJ, et al. Endovascular edge-to-edge mitral valve repair: short-term results in a porcine model. *Circulation*. 2003;108:1990–3.
48. Feldman T, Kar S, Rinaldi M, Fail P, Hermiller J, Smalling R, et al. Percutaneous mitral repair with the MitraClip system. Safety and midterm durability in the initial EVEREST (Endovascular Valve Edge-to-Edge REpair Study) cohort. *J Am Coll Cardiol*. 2009;54:686–94.
49. Hahn RT, Abraham T, Adams MS, Bruce CJ, Glas KE, Lang RM, et al. Guidelines for performing a comprehensive transesophageal echocardiographic examination: Recommendations from the American Society of Echocardiography and the Society of Cardiovascular Anesthesiologists. *Anesth Analg*. 2014;118:21–68.
50. Feldman T, Wasserman HS, Herrmann HC, Gray W, Block PC, Whitlow P, et al. Percutaneous mitral valve repair using the edge-to-edge technique: six-month results of the EVEREST Phase I Clinical Trial. *J Am Coll Cardiol*. 2005;46:2134–40.
51. Feldman T, Foster E, Glower DD, Glower DG, Kar S, Rinaldi MJ, et al. EVEREST II Investigators. Percutaneous repair or surgery for mitral regurgitation. *N Engl J Med*. 2011;364:1395–406.
52. Maisano F, Franzen O, Baldus S, Schäfer U, Hausleiter J, Butter C, et al. Percutaneous mitral valve interventions in the real world: Early and 1-year results from the ACCESS-EU. A prospective, multicenter, nonrandomized post-approval study of the MitraClip therapy in Europe. *J Am Coll Cardiol*. 2013;62:1052–61.
53. Eggebrecht H, Schelle S, Puls M, Plicht B, Von Bardeleben RS, Butter C, et al. Risk and outcomes of complications during and after MitraClip implantation: experience in 828 patients from the German TRANScatheter Mitral valve Interventions (TRAMI) registry. *Catheter Cardiovasc Interv*. 2015;86:728–35.
54. Capodanno D, Adamo M, Barbanti M, Giannini C, Laudisa ML, Cannata S, et al. Predictors of clinical outcomes after edge-to-edge percutaneous mitral valve repair. *Am Heart J*. 2015;170:187–95.
55. Rodríguez-Santamarta M, Estévez-Loureiro R, Gualis J, Alonso D, Pérez de Prado A, Fernández-Vázquez F. Reparación valvular mitral con dispositivo MitraClip® en paciente con insuficiencia mitral aguda tras infarto de miocardio. *Rev Esp Cardiol*. 2015;68:259–61.
56. D'Ascenzo F, Moretti C, Marra WG, Montefusco A, Omede P, Taha S, et al. Meta-analysis of the usefulness of MitraClip in patients with functional mitral regurgitation. *Am J Cardiol*. 2015;116:325–31.
57. Beigel R, Wunderlich NC, Kar S, Siegel RJ. The evolution of percutaneous mitral valve repair therapy. *J Am Coll Cardiol*. 2014;64:2688–700.
58. Attizzani GF, Ohno Y, Capodanno D, Cannata S, Dipasqua F, Immé S, et al. Extended use of percutaneous edge-to-edge mitral valve repair beyond EVEREST (Endovascular Valve Edge-to-Edge Repair) criteria: 30-day and 12-month clinical and echocardiographic outcomes from the GRASP (Getting Reduction of Mitral Insufficiency by Percutaneous Clip Implantation) registry. *JACC Cardiovasc Interv*. 2015;8:74–82.
59. Boekstegers P, Hausleiter J, Baldus S, Von Bardeleben RS, Beucher H, Butter C, et al. Percutaneous interventional mitral regurgitation treatment using the MitraClip system. *Clin Res Cardiol*. 2014;103:85–96.
60. Samim M, Stella PR, Agostoni P, Kluin J, Ramjankhan F, Budde RP, et al. Automated 3D analysis of pre-procedural MDCT to predict annulus plane angulation and C-arm positioning: benefit on procedural outcome in patients referred for TAVR. *JACC Cardiovasc Imaging*. 2013;6:238–48.
61. Nishimura RA, Otto CM, Bonow RO, Carabello BA, Erwin JP, Guyton RA, et al. 2014 AHA/ACC guideline for the management of patients with valvular heart disease: A report of the American College of Cardiology/American Heart Association Task Force on Practice Guidelines. *J Am Coll Cardiol*. 2014;63:e57–185.
62. Martín M, Mesa D, Carrasco F, Ruiz M, Delgado M, Suárez de Lezo J. Insuficiencia mitral tras MitraClip: impacto de la morfología del orificio regurgitante mitral evaluado mediante ecocardiografía tridimensional. *Rev Esp Cardiol*. 2014;67:581–2.
63. Foster E, Wasserman HS, Gray W, Homma S, Di Tullio MR, Rodriguez L, et al. Quantitative assessment of severity of mitral regurgitation by serial echocardiography in a multicenter clinical trial of percutaneous mitral valve repair. *Am J Cardiol*. 2007;100:1577–83.
64. Hamilton-Craig C, Strugnell W, Gaikwad N, Ischenko M, Speranza V, Chan J, et al. Quantitation of mitral regurgitation after percutaneous MitraClip repair: comparison of Doppler echocardiography and cardiac magnetic resonance imaging. *Ann Cardiothorac Surg*. 2015;4:341–51.
65. Lin BA, Forouhar AS, Pahlevan NM, Anastassiou CA, Grayburn PA, Thomas JD, et al. Color Doppler jet area overestimates regurgitant volume when multiple jets are present. *J Am Soc Echocardiogr*. 2010;23:993–1000.
66. Baumgartner H, Hung J, Bermejo J, Chambers JB, Evangelista A, Griffin BP, et al. Echocardiographic assessment of valve stenosis: EAE/ASE recommendations for clinical practice. *J Am Soc Echocardiogr*. 2009;22:1–23.
67. Bargiggia GS, Tronconi L, Sahn DJ, Recusani F, Raisaro A, De Servi S, et al. A new method for quantitation of mitral regurgitation based on color flow Doppler imaging of flow convergence proximal to regurgitant orifice. *Circulation*. 1991;84:1481–9.
68. Siegel RJ, Biner S, Rafique AM, Rinaldi M, Lim S, Fail P, et al. The acute hemodynamic effects of mitralclip therapy. *J Am Coll Cardiol*. 2011;57:1658–65.
69. Mauri L, Foster E, Glower DD, Apruzzese P, Massaro JM, Herrmann HC, et al. 4-year results of a randomized controlled trial of percutaneous repair versus surgery for mitral regurgitation. *J Am Coll Cardiol*. 2013;62:317–28.
70. Biaggi P, Felix C, Gruner C, Herzog BA, Hohlfeld S, Gaemperli O, et al. Assessment of mitral valve area during percutaneous mitral valve repair using the MitraClip system comparison of different echocardiographic methods. *Circ Cardiovasc Imaging*. 2013;6:1032–40.
71. Silvestry FE, Rodriguez LL, Herrmann HC, Rohatgi S, Weiss SJ, Stewart WJ, et al. Echocardiographic guidance and assessment of percutaneous repair for mitral regurgitation with the valve MitraClip: lessons learned from EVEREST I. *J Am Soc Echocardiogr*. 2007;20:1131–40.

72. Delgado V, Tops LF, Schuijf JD, De Roos A, Brugada J, Schalij MJ, et al. Assessment of mitral valve anatomy and geometry with multislice computed tomography. *JACC Cardiovasc Imaging*. 2009;2:556–65.
73. Bapat V, Buellesfeld L, Peterson MD, Hancock J, Reineke D, Buller C, et al. Transcatheter mitral valve implantation (TMVI) using the Edwards FORTIS device. *EuroIntervention*. 2014;10 Suppl U:U120–8.
74. Abdul-jawad Altisent O, Dumont E, Dagenais FF, Sénéchal M, Bernier M, O'Connor K, et al. Transcatheter mitral valve implantation with the FORTIS device: insights into the evaluation of device success. *JACC Cardiovasc Interv*. 2015;8:994–5.
75. Cheung A, Stub D, Moss R, Boone RH, Leipsic J, Verheye S, et al. Transcatheter mitral valve implantation with Tiara bioprosthesis. *EuroIntervention*. 2014;10 Suppl U:U115–9.
76. Gurvitch R, Wood DA, Leipsic J, Tay E, Johnson M, Ye J, et al. Multislice computed tomography for prediction of optimal angiographic deployment projections during transcatheter aortic valve implantation. *JACC Cardiovasc Interv*. 2010;3:1157–65.
77. Blanke P, Naoum C, Webb J, Dvir D, Hahn RT, Grayburn P, et al. Multimodality imaging in the context of transcatheter mitral valve replacement: establishing consensus among modalities and disciplines. *JACC Cardiovasc Imaging*. 2015;8:1191–208.
78. Chen S, Zhu Q, Ning Z, Wu Y, Zhang Z, Li X. Multidetector computed tomography angiography combined with intravascular ultrasound for the evaluation of coronary veins for percutaneous mitral annulus repair using transcatheter sinus devices. *Echocardiography*. 2015;32:1851–7.
79. Van Bibber R, Hoppe U, Schofer J, Haude M, Herrman J, Vainer J, et al. The relationship of cardiac veins to mitral annulus allows for percutaneous mitral annuloplasty in most patients: MSCT analysis from the AMADEUS trial. *Eur Heart J*. 2008;29:580.